Supporting Information of

A novel benzothiadiazole-based and NIR-emissive fluorescent sensor for detection of Hg^{2+} and its application in living cells and zebrafish imaging

Haifeng He[a], Xiangying Meng[a], Lili Deng[a], Qi Sun[c], Xuelong Huang[b]*, Ning Lan[b], Feng Zhao[a]*

[a]*Jiangxi Engineering Laboratory of Waterborne Coating, School of Chemistry and Chemical Engineering, Jiangxi Science and Technology Normal University, Nanchang 330013, People's Republic of China*

[b] *College of Pharmacy, Gannan Medical University, Ganzhou 341000, People's Republic of China*

[c]*Key Laboratory for Green Chemical Process of Ministry of Education and School of Chemistry and Environmental Engineering, Wuhan Institute of Technology, Wuhan,*

430205, PR China

* Corresponding author E-mail: huangxuelong1988@126.com; zhf19752003@163.com

S1. General information

Unless stated otherwise, all analytical grad chemicals and solvents used in this paper were purchased from commercial vendors. The salts used in stock solutions of metal ions were Na_2SO_4, KNO_3, $AgNO_3$, $Pb(NO_3)_2$, $CoSO_4·7H_2O$, $ZnSO_4·7H_2O$, $MgSO_4$, $NiSO_4·6H_2O$, $CuSO_4·5H_2O$, $FeSO_4·7H_2O$, $MnSO_4·2H_2O$, $Cr(NO_3)_3·9H_2O$, $Al(NO_3)_3·9H_2O$, $Fe(NO_3)_3·9H_2O$ and $Hg(ClO_4)_2·3H_2O$. Various anions were prepared by NaCl, NaBr, NaOH, NaF, Na_2CO_3, $NaNO_2$, $NaHCO_3$, NaH_2PO_4, Na_2HPO_4, $NaNO_3$, Na_2S, Na_2SO_3, $NaHSO_3$, $NaSO_4$, CH_3COONa.The ^1H and ^{13}C NMR spectra were collected on a Bruker AV-400(400 MHz) in a DMSO-d_6 solution with TMS as the internal standard. Mass spectrometry was recorded with a Finnigan LCQ mass spectrometer and an Agient 1200 LC/MSD mass spectrometer, and signals were given in m/z. Elemental analysis (**EA**) was obtained on a Vario ELIII CHNSO elemental analyzer. UV–vis absorption spectra were recorded on a Perkin Elmer Lambda-900 spectrophotometer. Fluorescence spectra was determined by a Hitachi F-4600 fluorescence spectrophotometer. Photoluminescence (PL) quantum yields were carried out using a Hamamatsu system for absolute PL quantum yield measurements (type C11347).

S2. Synthesis of compounds

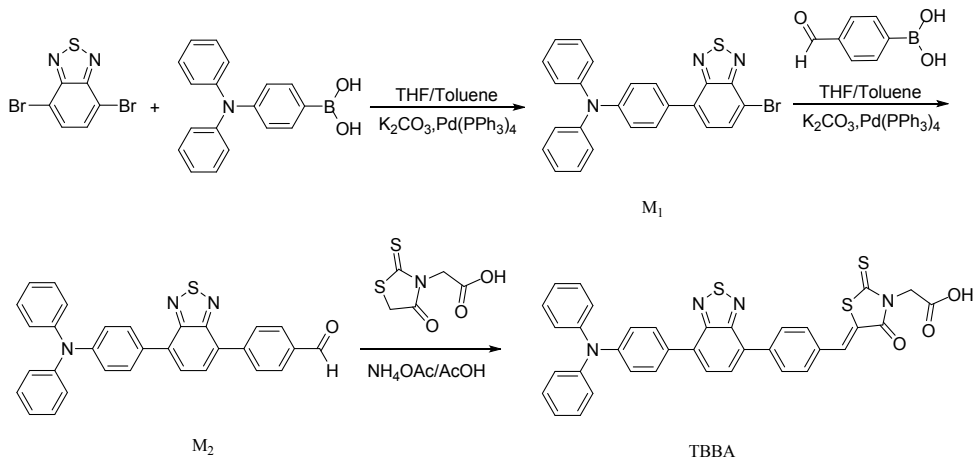

Scheme S1. The synthetic pathways of probe **TBBA**

S 2.1 Synthesis of compound 4-(7-bromobenzo[c][1,2,5]thiadiazol-4-yl)-N,N-diphenylaniline (M1)

The synthesis of the chemosensor **TBBA** was carried out by a palladium-catalyzed Suzuki reaction(Scheme 1). 4,7-dibromobenzo[c][1,2,5]thiadiazole(291.8 mg, 1 mmol) and (4-(diphenylamino)phenyl)boronic acid (289.1mg, 1 mmol) were mixed with tetrakis(triphenylphosphine)palladium(0) ($Pd(PPh_3)_4$, 3 mol%) in a mixture of potassium carbonate(20% wt/v aqueous solution, 2 mL), toluene (16 mL) and DCM (8 mL) under argon. The reaction mixture was vigorously stirred at 90 ℃ for 8 h and then cooled to room temperature. The mixture was poured into deionized water (100 mL) and extracted with dichloromethane. After that, the organic layer was washed with water and dried over anhydrous $MgSO_4$. The solvent was then evaporated, and the product was purified by column chromatography on silica with petroleumether/ethyl acetate (25/1 in v/v) as the eluent to give the target compound M1. ^{1}H NMR (400 MHz, $CDCl_3$): δ (ppm) = 7.89 (d, *J* = 8 Hz, 1H), 7.80 (d, *J* = 8 Hz, 2H), 7.54 (d, *J* = 8 Hz, 1H), 7.29 (t, *J* = 8 Hz, 4H), 7.20-7.17 (m, 6H), 7.08 (t, *J* = 6 Hz, 2H). ^{13}C NMR (100 MHz, $CDCl_3$): δ (ppm) = 154.0, 153.2, 148.5, 147.4, 133.6, 132.4, 129.9, 129.4, 127.3, 125.1, 124.2, 123.5, 122.6, 112.2. EI-MS: m/z = 457.10. Anal. Calcd. for $C_{24}H_{16}BrN_3S$: C, 62.89; H, 3.52; N, 9.17. Found: C, 62.81; H, 3.47; N, 9.26.

S 2.2 Synthesis of compound 4-(7-(4-(diphenylamino)phenyl)benzo[c][1,2,5]thiadiazol-4-yl)

benzaldehyde (M2)

Compound M1 (228 mg, 0.5 mmol), 4-formylphenylboronic acid (75 mg, 0.5 mmol), potassium carbonate(20% wt/v aqueous solution, 1 mL) and $Pd(PPh_3)_4$ (3 mol%) were dissolved in the mixture of DCM (8 mL) and toluene (16mL). The mixture was stirred 6 h at 80 ℃. The solvent was then evaporated and the product was purified by column chromatography on silica with petroleumether/ethyl acetate (10/1 in v/v) as the eluent. The solvent was evaporated and compound M2 was obtained. ^{1}H NMR (400 MHz, $CDCl_3$): δ (ppm) = 10.01 (s, 1H), 8.07 (d, *J* = 8.1 Hz, 2H), 7.95 (d, *J* = 8.2 Hz, 2H), 7.80 (d, *J* = 8.6 Hz, 2H), 7.75 (d, *J* = 7.4 Hz, 1H), 7.69 (t, *J* = 6.3 Hz, 1H), 7.21 (t, *J* = 7.8 Hz, 5H), 7.11 (t, *J* = 8.1 Hz, 5H), 6.99 (d, *J* = 7.3 Hz, 2H); ^{13}C NMR (100 MHz, $CDCl_3$): δ (ppm) =191.82, 154.04, 153.87, 148.42, 147.36, 143.42, 135.73, 134.12, 130.88, 130.02, 129.90, 129.74, 129.37, 128.98, 126.92, 125.04, 123.49, 122.59. HRMS: m/z = 483.14035.

S2.3 Synthesis of compound 2-(5-(4-(7-(4-(diphenylamino)phenyl)benzo[c][1,2,5]thiadiazol-4-yl)benzylidene)-4-oxo-2-thioxothiazolidin-3-yl)acetic acid (TBBA)

Compound M2 (521.6 mg, 1.08 mmol) and rhodanine-3-acetic acid (203.3mg, 1.07 mmol) were added into the acetic acid (25 mL) in the presence of ammonium acetate (83mg) under nitrogen atmosphere. The mixture was stirred 24h at 100 ℃. After the mixture cooled to room temperature, the reaction was quenched using ice water. The precipitate was filtered and washed thoroughly with water. The solvent was then evaporated, and the product was purified by column chromatography on silica with petroleumether/ethyl acetate (1/1 in v/v) as the eluent. The solvent was evaporated, and compound TBBA was obtained. **^{1}H NMR** (400 MHz, DMSO-d_6) δ (ppm) 8.24 (d, *J*=8 Hz, 2H, -ArH), 8.04 (d, *J*=4 Hz, 1H, vinyl H), 7.92-7.98 (m, 4H, -ArH), 7.83 (d, *J*=8 Hz, 2H, -ArH), 7.35-7.38 (m, 4H, -ArH), 7.11-7.13 (m, 8H, -ArH), 4.77(s, 2H, $-CH_2$). **^{13}C NMR** (100 MHz, DMSO-d_6) δ= 193.76, 167.86, 167.04, 157.13, 154.69, 154.00, 148.33, 147.48, 139.94, 134.00, 133.33, 133.13, 131.66, 130.87, 130.57, 130.34, 129.69, 127.92, 125.27, 124.32, 122.73, 121.20, 115.36, 45.77. HRMS: m/z = 656.10131.

S3. Calculations

S3.1 Determination of Quantum Yield

The fluorescence quantum yield was deduced by the following equation[1],

$$\Phi_x = \Phi_s \times \frac{D_x}{D_s} \times \frac{A_s}{A_x} \times \frac{{\eta_x}^2}{{\eta_s}^2}$$

Here the relative quantum yield of the probe and probe metal complex was determined by using fluorescein as standard fluorescence mean, with quantum yield of Φ_{ref} = 0.90 (in NaOH). Where the notations in the above equation such that, Φ is the fluorescence quantum yield, D is the area under the emission spectra at λ_{em}= 446 nm, A is the absorbance at the excitation wavelength λ_{ex} = 350 nm, x subscript denotes unknown compound, and s as standard reference and η is the refractive index of the solvents used.

S3.2 Determination of Stoichiometry by Continuous Variation Plot (Job's plot) Measurement

The stoichiometric binding ratio of probe **TBBA** and Hg^{2+} ion was confirmed by continuous variation emission analysis[2] at λ_{em} 675 nm, the resulting data was plotted as change in fluorescence intensity, emission intensity in the vertical axis against the mole fraction, $X_{Hg^{2+}}$ of Hg^{2+} ions in the horizontal axis.

S3.3 Determination of Binding Constant

The binding constant of the **TBBA + Hg^{2+}** complex formed in solution has been determined by using the standard Benesi-Hildebrand (B-H) equation[2].

$$\frac{1}{F - F_o} = \frac{1}{K_a(F_{max} - F_o)\,[Hg^+]} + \frac{1}{F_{max} - F_o}$$

Where, F_o is the fluorescence intensity of free probe **TBBA**, F is the observed fluorescence intensity at any given concentration of Hg^{2+}, F_{max} is the intensity at saturation point with the Hg^{2+}, K_a is the association constant and [Hg^{2+}] is the concentration of the Hg^{2+} ions in micromolar.

S3.4 Determination of Detection Limit

The detection limit was calculated based on fluorescence titration as a function the solubility of Hg^{2+} at **λ_{em}** 446 nm. The fluorescence emission spectrum of free probe **TBBA** was measured over 3 times to determine standard deviation for blank measurement. A linear plot was constructed with average values of the intensities against the concentration of Hg^{2+} ions for determining the slope. Using the slope the detection limit was calculated from the following equation[2-3].

$$LOD = \frac{3\sigma}{K}$$

where, σ is the standard deviation of the blank solution and K is the slope between intensity versus sample concentration.

S4. **Cell Cultures and Imaging**

A549 Cells were obtained from Wuhan Institute of Technology, and cultured in Dulbecco's modified Eagle's medium (DMEM) supplemented with 10% fetal bovine serum and penicillin-streptomycin ($0.5U \cdot mL^{-1}$ of penicillin and $0.5\ g \cdot mL^{-1}$ strepomycin) on a cell culture flask at 37℃ in an atmosphere of air with 5% CO_2 and constant humidity. Each cell line was seeded in a 6-well plate for 24 h. The cells were initially incubated with **TBBA** (10 μM) in culture medium for 30 min at 37℃. After washing three times with PBS to remove the remaining **TBBA**, the A549 cells were incubated in the absence and presence of Hg^{2+} (25 and 50 μM) in culture medium for another 30 min at 37 ℃. The imaging was carried out using inverted fluorescence microscopy (Olympus IX71, Japan).

S5. **Imaging of Zebrafish**

The 3-7 days old zebrafishes postfertilization were purchased from Eze-Rinka Company (Nanjing, China). The zebrafishes were cultured in 5mL of embryo medium supplemented with 1-phenyl-2-thiourea (PTU) in 6-well plates for 24h at 30℃. Zebrafishes were divided into two groups and both incubated with **TBBA** (10 μM) for 1h. After washing three times to remove the remaining **TBBA**, one group as control group and other group further treated with Hg^{2+} (100 μM) for another 1 h. The fluorescence images were acquired with stereo microscopy (Olympus SZX16, Japan).

LIVE SUBJECT STATEMENT:
All experiments were performed in accordance with the Guidelines "Declaration of Helsinki Principles", and approved by the ethics committee at "Gannan Medical University".

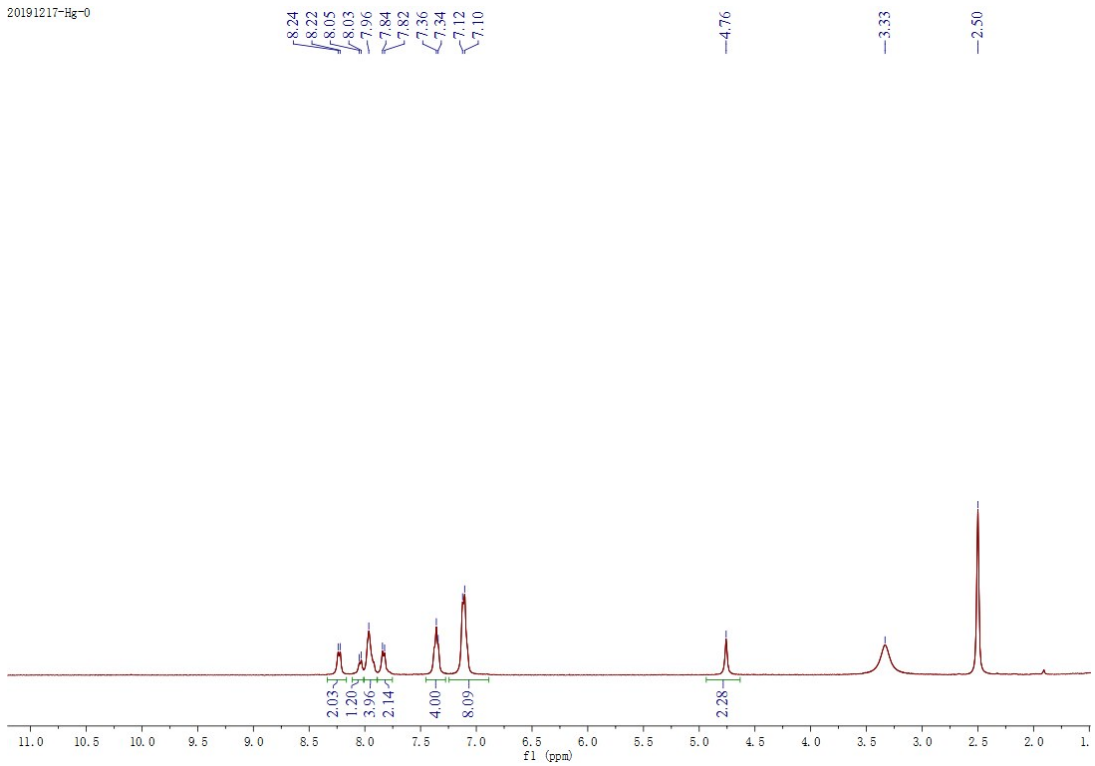

Figure S1. ^{1}**H NMR** Spectrum of probe **TBBA** in DMSO-d_6

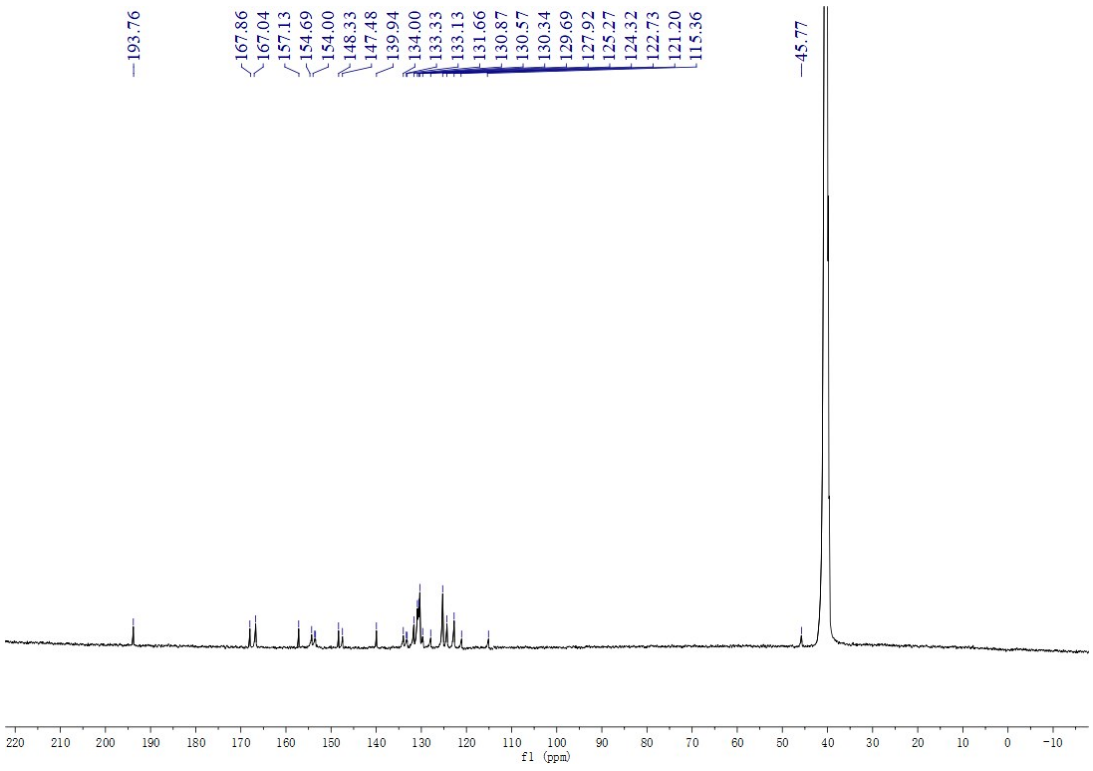

Figure S2. ^{13}**C NMR** Spectrum of probe **TBBA** in DMSO-d_6

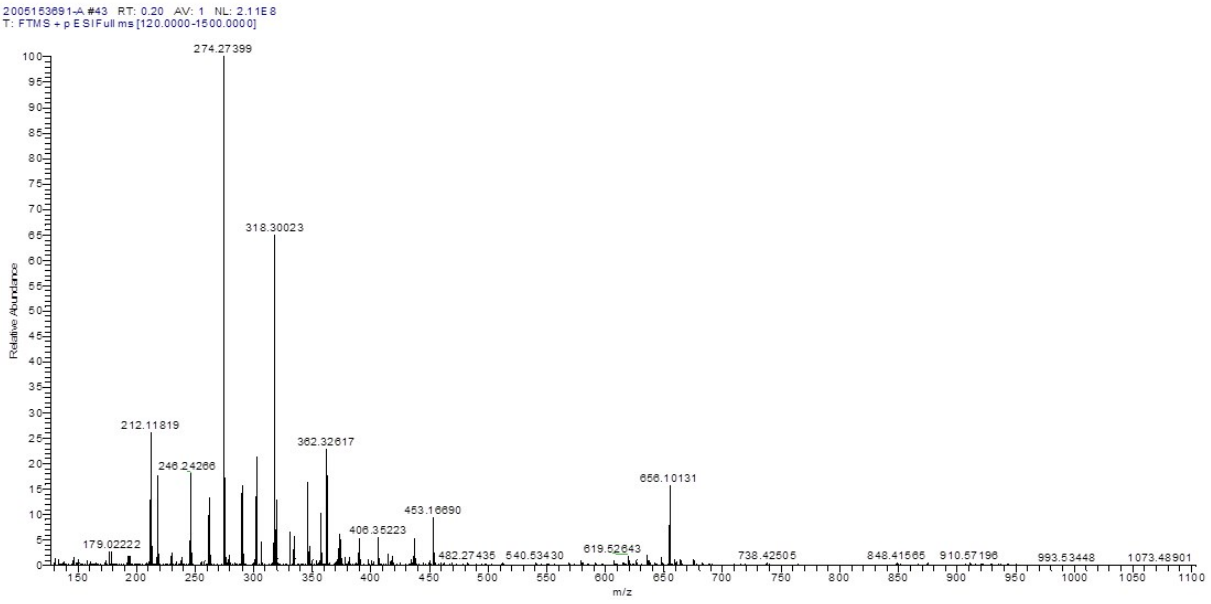

Figure S3 HRMS spectrum of **TBBA**

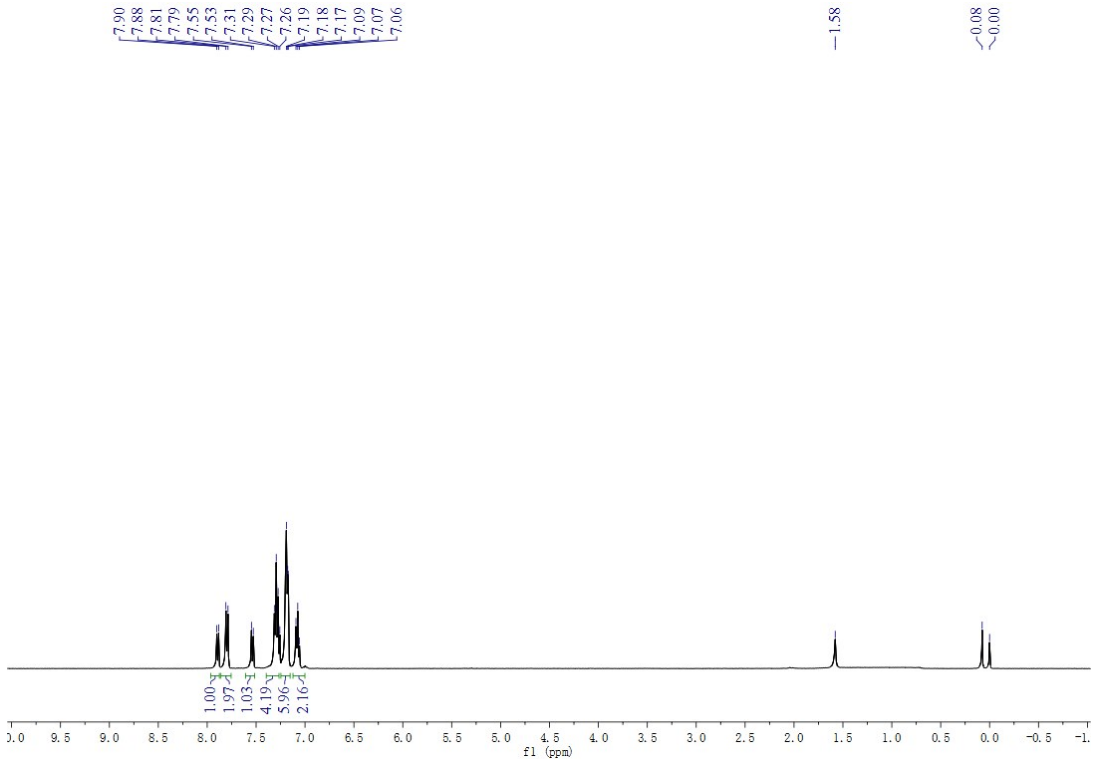

Figure S4. ^{1}H NMR Spectrum of intermediate **M1** in $CDCl_3$

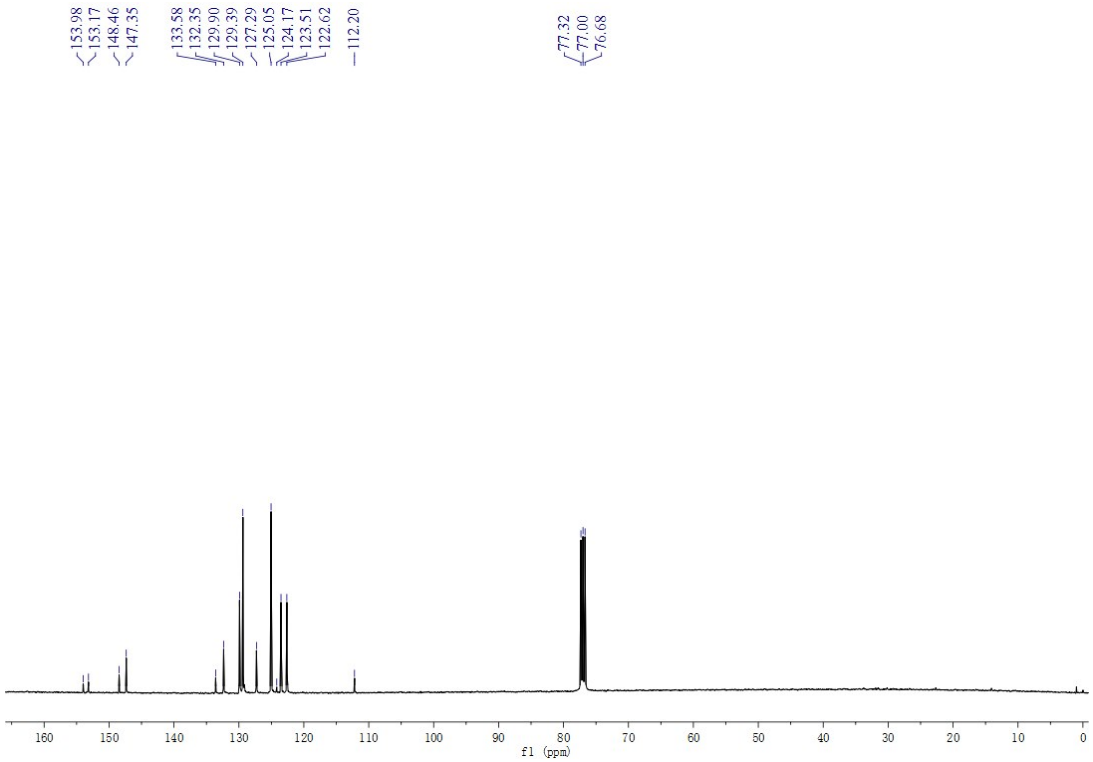

Figure S5. ^{13}**C NMR** Spectrum of intermediate **M1** in $CDCl_3$

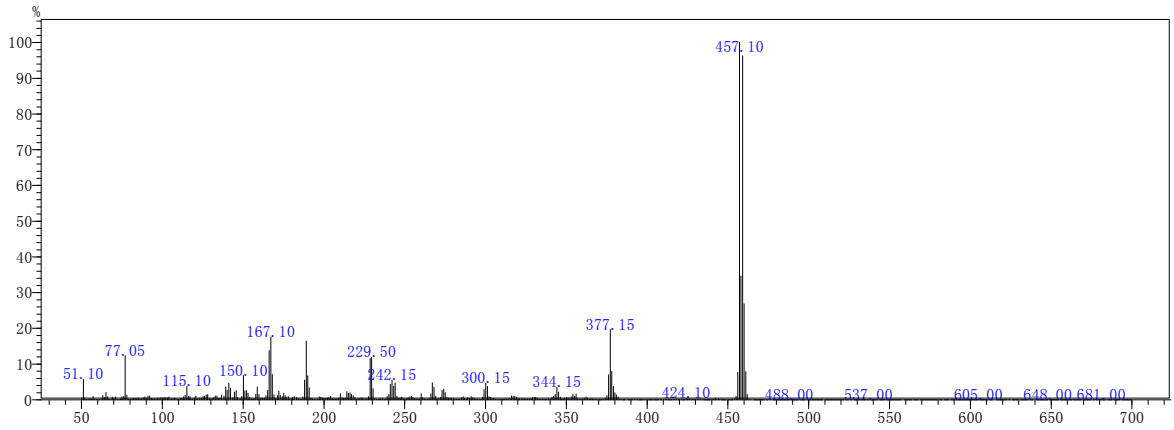

Figure S6 EI-MS spectrum of intermediate **M1**

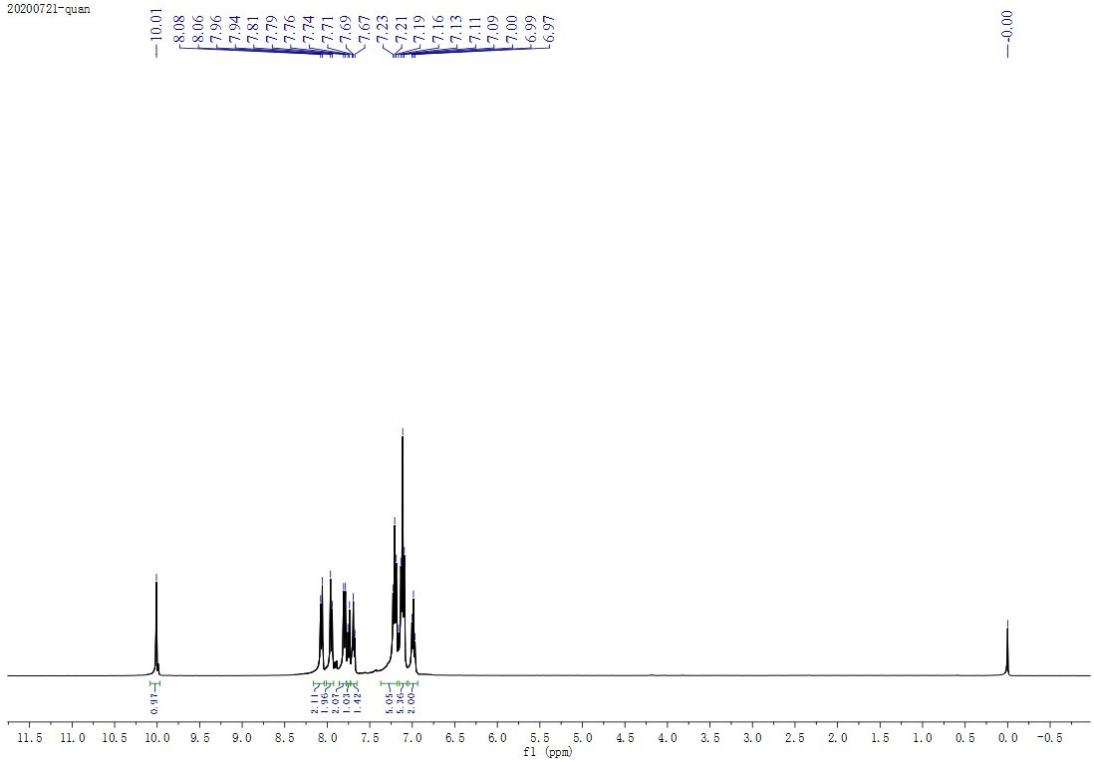

Figure S7. ^{1}H NMR Spectrum of intermediate **M2** in $CDCl_3$

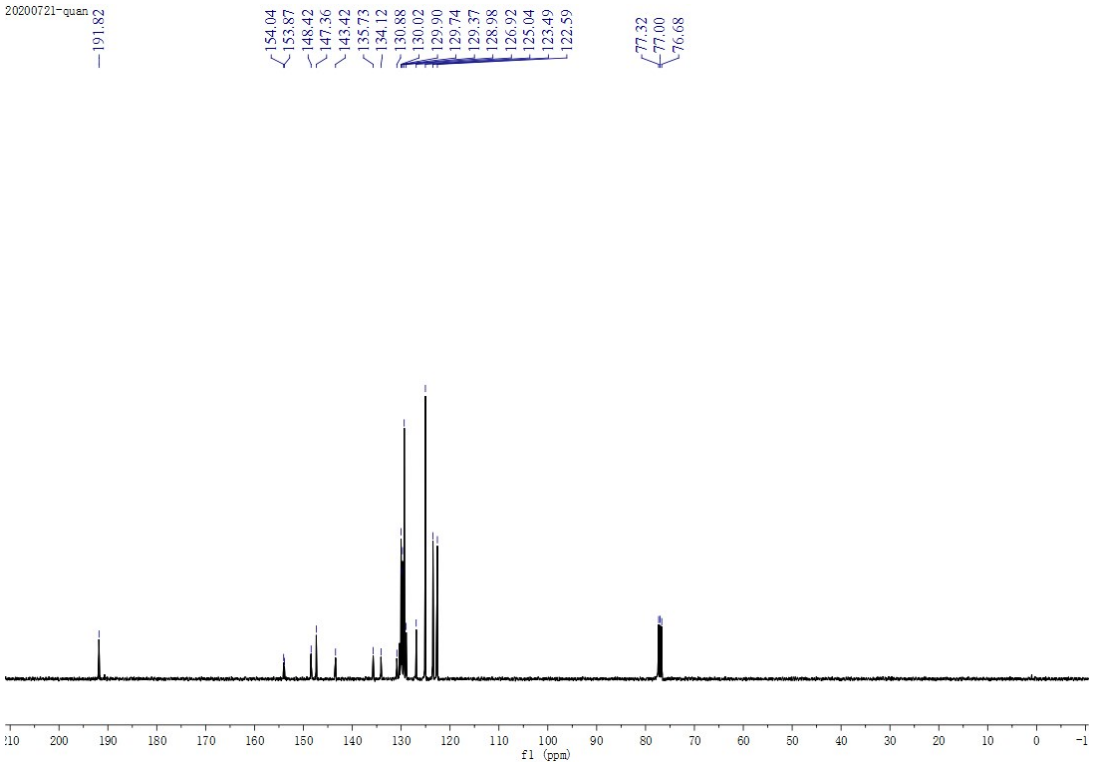

Figure S8. ^{13}C NMR Spectrum of intermediate **M2** in $CDCl_3$

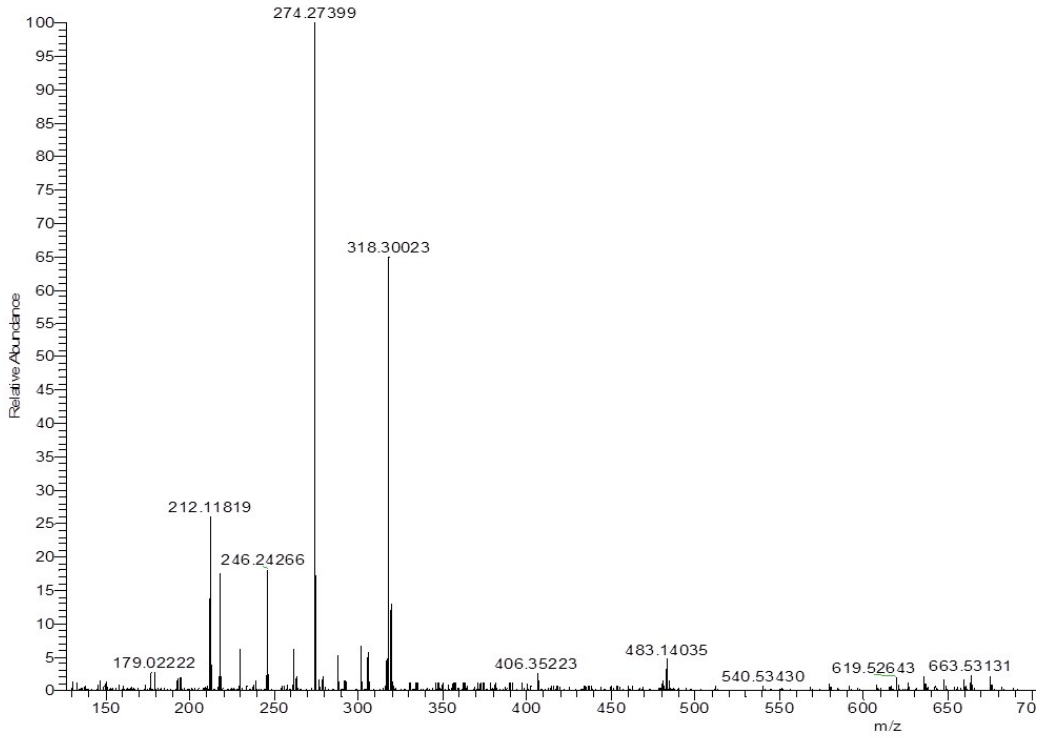

Figure S9 HRMS spectrum of intermediate **M1**.

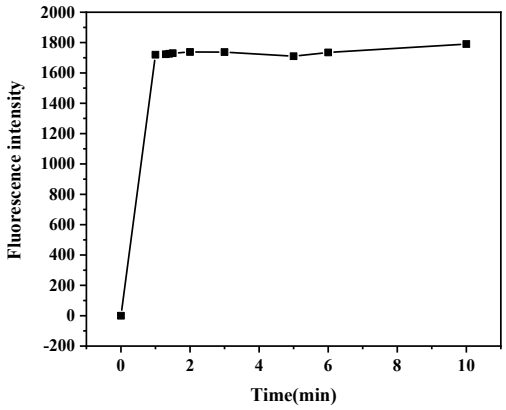

Figure S10. Effect of response time on the fluorescence intensity of **TBBA** (20 μM) in the presence of 80 μM Hg^{2+}

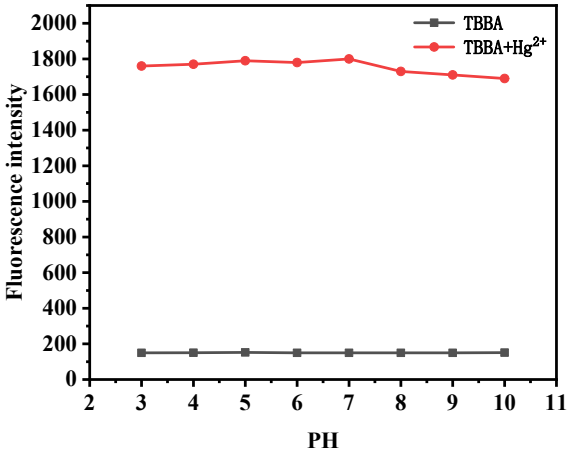

Figure S11. Fluorescence of probe TBBA (20 μM) and TBBA-Hg^{2+} at different pH.

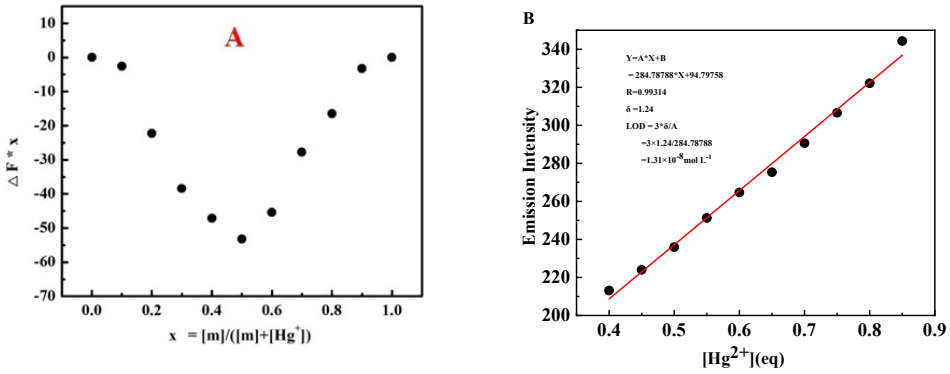

Figure S12 (A) Job's plot for the complex of TBBA with Hg^{2+}; (B) The limit of detection (LOD) is 13.1 nM.

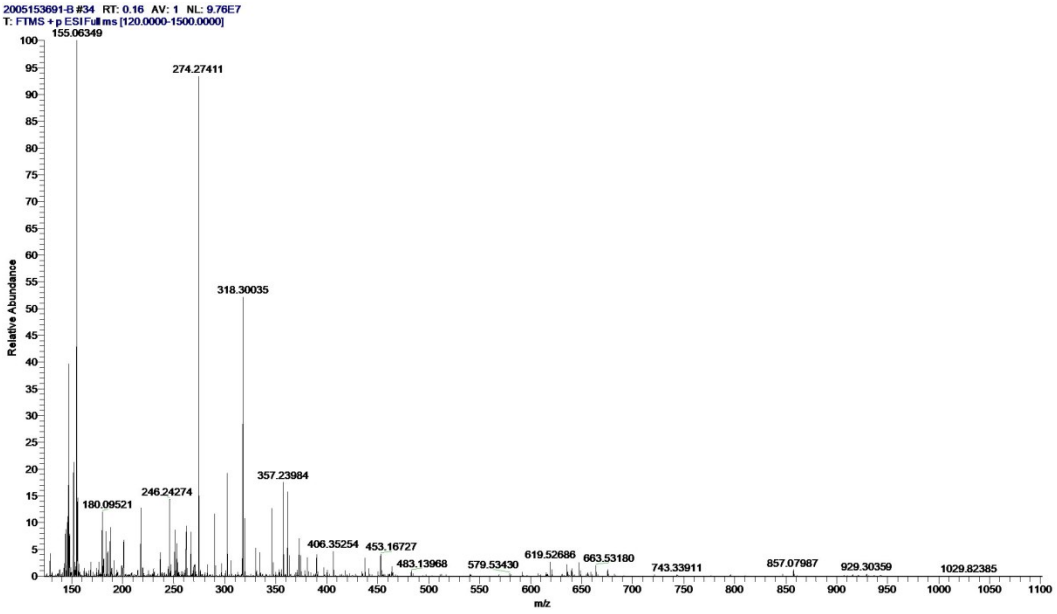

Figure S13 ESI-MS spectrum of TBBA in the presence of 3 equiv. Hg^{2+}.

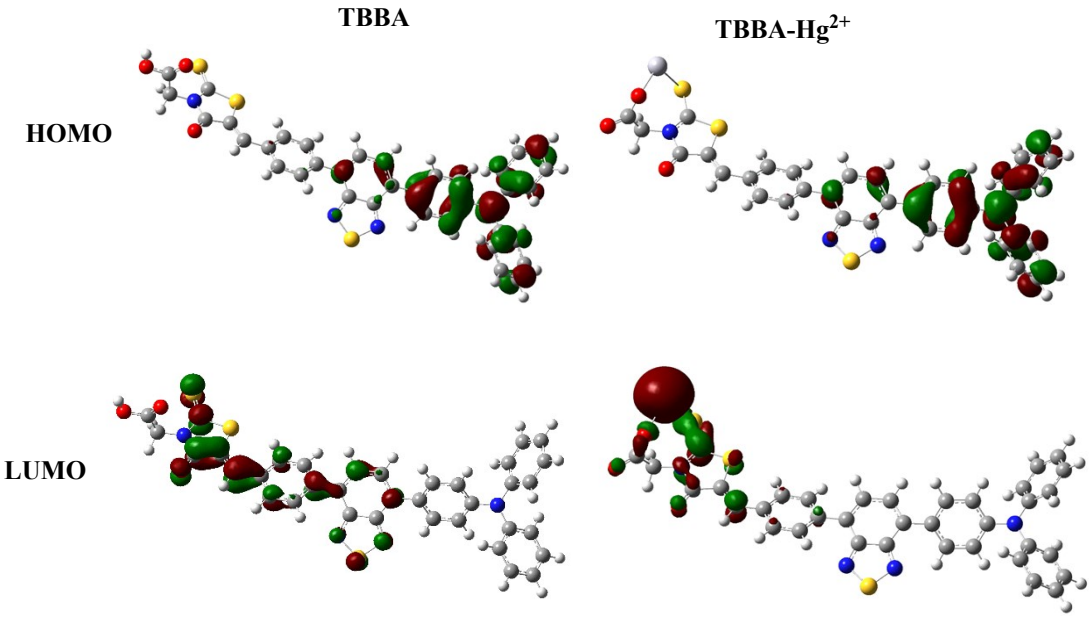

Figure S14 HOMO−LUMO energy diagrams of TBBA with Hg^{2+} ions.

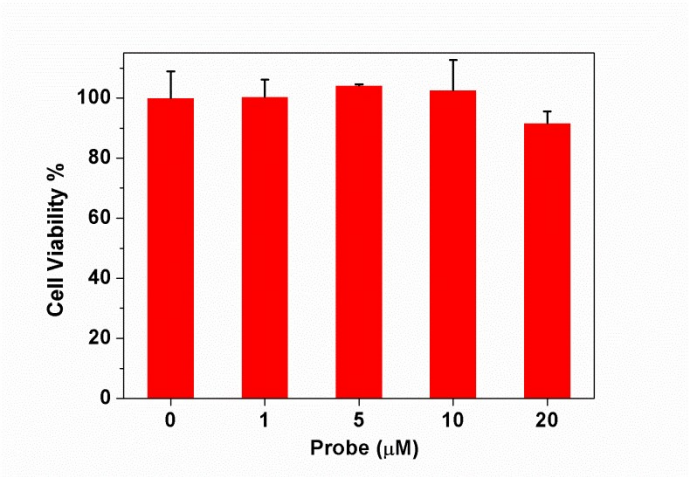

Figure S15. The cytotoxicity of TBBA against normal cells incubated with different concentration of **TBBA** for 24 h

Table 1 Comparison on detection limits of reported fluorescent sensor for Hg^{2+} ion.

Probes	λ_{em} (nm)	λ_{ex} (nm)	Stocks shift(nm)	LOD	Cell imaging	Zebrafish experiment	References in main manuscript
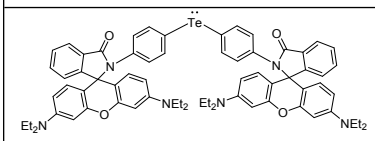	582	515	67	1.71μM	No	No	4
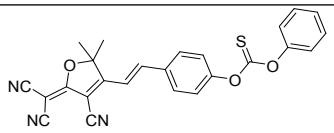	604	560	44	17 nM	No	No	5
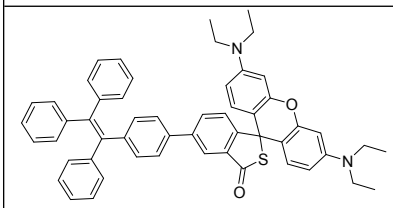	592	355	237	43pM	No	No	6
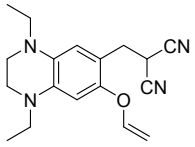	625	475	150	7.1 nM	Yes	Yes	7
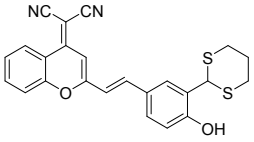	659	514	145	68nM	Yes	No	

							8
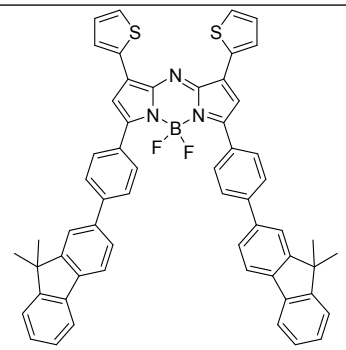	750	650	100	2.51μM	No	No	9
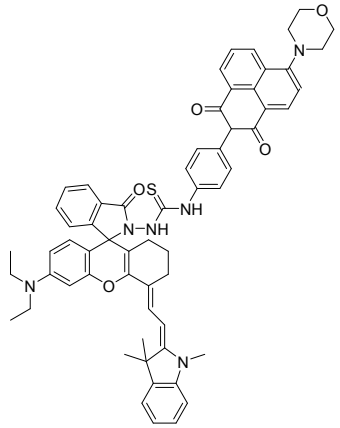	746	670	76	1.91×10^{-7} M	No	No	10
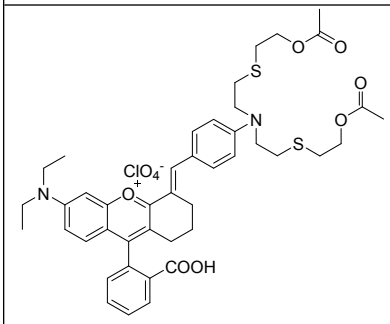	661	500	161	9.95nM	Yes	No	11
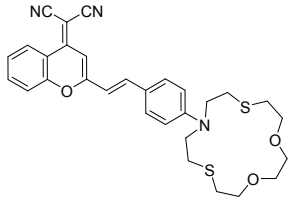	645	517	128	0.14μM	Yes	Yes	12

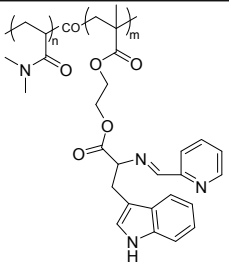	364, 464	285	79	4.71nM	No	No	13
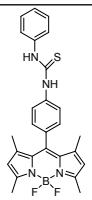	529	319	210	2.4μM	Yes	Yes	14
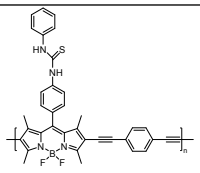	615	470	145	0.22 μM	Yes	Yes	14
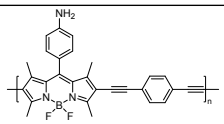	618	470	148	2.86 μM	Yes	No	14
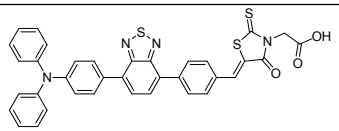	657	480	177	13.1nM	Yes	Yes	This work

References

1. (a)S.-J. Li, Y.-J. Fu, C.-Y. Li, Y.-F. Li, L.-H. Yi and J. Ou-Yang, *Anal. Chim. Acta*, 2017, **994**, 73-81; (b)E. Bozkurt, M. Arık and Y. Onganer, *Sensor Actuat B-Chem.*, 2015, **221**, 136-147.
2. (a)Y. Li, J. Wu, X. Jin, J. Wang, S. Han, W. Wu, J. Xu, W. Liu, X. Yao and Y. Tang, *Dalton Trans.*, 2014, **43**, 1881-1887; (b)M. Ahumada, E. Lissi, A. M. Montagut, F. Valenzuela-Henríquez, N. L. Pacioni and E. I. Alarcon, *Analyst*, 2017, **142**, 2067-2089.
3. M. Shortreed, R. Kopelman, M. Kuhn and B. Hoyland, *Anal. Chem.*, 1996, **68**, 1414-1418.
4. A. A. Soares-Paulino, L. Giroldo, G. Celante, C. Lodeiro and A. A. Dos Santos, *Dyes Pigm.*, 2018, **159**, 121-127.
5. J. Xu, Z. Wang, C. Liu, Z. Xu, N. Wang, X. Cong and B. Zhu, *Luminescence*, 2018, **33**, 1122-1127.
6. Y. Jiang, Q. Duan, G. Zheng, L. Yang, J. Zhang, Y. Wang, H. Zhang, J. He, H. Sun and D. Ho, *Analyst*, 2019, **144**, 1353-1360.
7. L. Yang, Y. Su, Y. Geng, H. Xiong, J. Han, Q. Fang and X. Song, *Org. Biomol. Chem.*, 2018, **16**, 5036-5042.
8. L. Huang, Z. Yang, Z. Zhou, Y. Li, S. Tang, W. Xiao, M. Hu, C. Peng, Y. Chen, B. Gu and H. Li, *Dyes Pigm.*, 2019, **163**, 118-125.
9. S. Liu, Z. Shi, W. Xu, H. Yang, N. Xi, X. Liu, Q. Zhao and W. Huang, *Dyes Pigm.*, 2014, **103**, 145-153.
10. S.-K. Yao, Y. Qian, Z.-Q. Qi, C.-G. Lu and Y.-P. Cui, *New J. Chem.*, 2017, **41**, 13495-13503.

11. X. Jiao, C. Liu, S. He, L. Zhao and X. Zeng, *Dyes Pigm.*, 2019, **160**, 86-92.
12. H. Lv, G. Yuan, G. Zhang, Z. Ren, H. He, Q. Sun, X. Zhang and S. Wang, *Dyes Pigm.*, 2020, **172**, 107658.
13. N. Choudhury, B. Ruidas, B. Saha, K. Srikanth, C. Das Mukhopadhyay and P. De, *Polym Chem.*, 2020, **11**, 2015-2026.
14. L. Xiao, Q. Sun, Q. Zhao and X. Cheng, *Anal. Bioanal. Chem.*, 2020, **412**, 881-894.